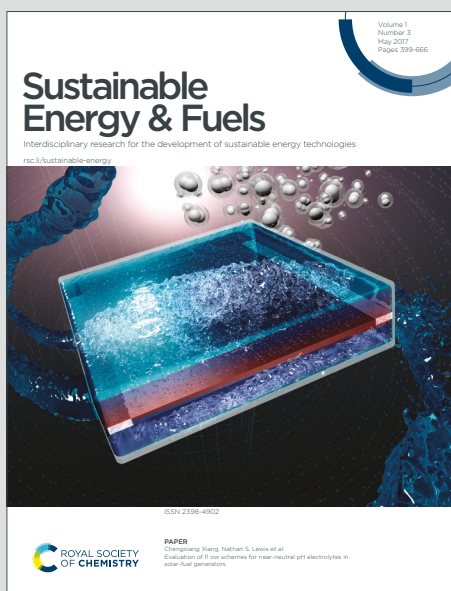


# Sustainable Energy & Fuels

Interdisciplinary research for the development of sustainable energy technologies

Accepted Manuscript

This article can be cited before page numbers have been issued, to do this please use: C. Tristán, M. Rumayor, A. Dominguez-Ramos, M. Fallanza, R. Ibáñez and I. Ortiz, *Sustainable Energy Fuels*, 2020, DOI: 10.1039/D0SE00372G.



This is an Accepted Manuscript, which has been through the Royal Society of Chemistry peer review process and has been accepted for publication.

Accepted Manuscripts are published online shortly after acceptance, before technical editing, formatting and proof reading. Using this free service, authors can make their results available to the community, in citable form, before we publish the edited article. We will replace this Accepted Manuscript with the edited and formatted Advance Article as soon as it is available.

You can find more information about Accepted Manuscripts in the [Information for Authors](#).

Please note that technical editing may introduce minor changes to the text and/or graphics, which may alter content. The journal's standard [Terms & Conditions](#) and the [Ethical guidelines](#) still apply. In no event shall the Royal Society of Chemistry be held responsible for any errors or omissions in this Accepted Manuscript or any consequences arising from the use of any information it contains.

1 **Life cycle assessment of salinity gradient energy recovery by reverse electro dialysis**  
2 **in a seawater reverse osmosis desalination plant**

3 Carolina Tristán, Marta Rumayor, Antonio Dominguez-Ramos, Marcos Fallanza,  
4 Raquel Ibáñez, Inmaculada Ortiz\*

5 **Abstract**

6 Salinity gradient energy capture by reverse electro dialysis (SGE-RED) can play a part in  
7 the shift away from fossil fuels towards a carbon-neutral renewable energy supply;  
8 however, likewise other renewable power technologies, SGE-RED environmental  
9 soundness hinge on its whole life-cycle environmental loads. This study surveys the Life  
10 Cycle Assessment of SGE-RED technology. We quantified (i) the environmental loads  
11 per 1.0 kWh generated by a stand-alone RED unit and then, (ii) the environmental burdens  
12 related to the energy provision from an up-scaled RED system to a seawater reverse  
13 osmosis (SWRO) desalination plant per 1.0 m<sup>3</sup> of desalted water. The RED unit's  
14 assessment results show SGE-RED is environmentally competitive with other renewable  
15 sources such as photovoltaics or wind. Regarding the component's contribution analysis,  
16 the spacer's fabric material drives the RED environmental burden as the number of cell

---

\* corresponding author: [ortizi@unican.es](mailto:ortizi@unican.es)

Department of Chemical and Biomolecular Engineering, University of Cantabria, Av. Los Castros 46,  
39005 Santander, Spain.

† Electronic supplementary information (ESI) available: RED stacks' electric parameters; RED stacks'  
inventory data; Gibbs free energy of mixing.

17 pairs is increased. The scaling-up of the RED unit, however, improves its full  
18 environmental profile. Preliminary results of SGE-RED combination with a SWRO plant  
19 suggest that the energy harnessed from SWRO's concentrate streams by RED could  
20 enhance the environmental performance of the desalination industry. Further research is  
21 required to identify SWRO-RED design alternatives that minimize the life cycle burden  
22 while still yielding good technical and economic performance.

23

View Article Online  
DOI: 10.1039/D0SE00372G

## 24 1. Introduction

25 Salinity gradient is an untapped renewable energy source envisaged as a candidate to  
26 advance the progressive decarbonisation of the current electric energy portfolio under  
27 particular technical conditions.<sup>1,2</sup> Reverse electrodialysis (RED) stands out among  
28 membrane-based technologies to harvest salinity gradient energy (SGE).<sup>1</sup> RED, the  
29 reverse of the conventional desalination process i.e. electrodialysis, is an electrochemical  
30 membrane process that makes use of ion-exchange membranes (IEM) to recover the  
31 energy released in the reversible mixing of two solutions with different salinities.<sup>2</sup> A RED  
32 unit is assembled by stacking a series of repeating units or cell pairs in a plate-and-frame  
33 arrangement. Each cell pair is comprised of an anion- and a cation-exchange membrane,  
34 with net polymer spacers placed in between to form the channels within the dilute and  
35 concentrate salt feed solutions flow. The chemical potential difference between the  
36 concentrate and dilute salt solutions gives rise to an electric potential difference over  
37 each membrane and drives the migration and diffusion of ions across membranes with  
38 opposing-charge functional groups, resulting in an ionic flux that is converted into an  
39 electron flux through redox reactions at the electrodes. The DC electric current and  
40 voltage yielded by the RED pile are readily accessible to power an external electric load  
41 connected to the RED electrodes.

42 RED performance has improved over the last decades, moving from relatively small  
43 power densities of  $0.05 \text{ W m}^{-2}$  reported in 1954 by Pattle<sup>3</sup> to  $6.70 \text{ W m}^{-2}$  recently obtained  
44 mixing synthetic NaCl solutions mimicking fresh or brackish water and concentrated  
45 brines at a temperature of  $60 \text{ }^\circ\text{C}$ .<sup>4</sup> Last research advances have stepped up RED  
46 Technology Readiness Level enabling the progress from lab-scale units<sup>5,6</sup> to up-scaled  
47 prototypes<sup>7-10</sup> and pilot plants.<sup>11,12</sup>

48 SGE can be obtained from natural or anthropogenic streams. The reclamation of industrial  
49 effluents in osmotic power generation plants as SGE-RED is a promising alternative to  
50 provide energy savings from an otherwise waste stream. Several authors have examined  
51 the energy recovery from desalination's concentrate effluents,<sup>13–18</sup> as well as secondary  
52 treated wastewater effluents.<sup>7,19,20</sup> Moreover, RED operation with high-salinity effluents  
53 delivers higher energy densities than seawater/river water pairs extensively tested in  
54 previous works.<sup>4,21,22</sup>

55 The ever-growing water demand, along with the steady decline of conventional water  
56 resources<sup>23</sup> is propelling the adoption of different water enhancement alternatives, such  
57 as desalination or water reclamation and reuse.<sup>24</sup> Recent figures about desalination sector  
58 signify this trend. The global installed desalination capacity has been growing steadily at  
59 an average rate of 8% per year since 1965 accounting for 97.4 million cubic meters per  
60 day ( $\text{Mm}^3 \text{d}^{-1}$ ) in 2017 and over 20,000 desalination plants had been contracted so far  
61 around the world.<sup>24</sup>

62 Among membrane technologies, reverse osmosis (RO) leads the global market for  
63 seawater desalination sharing 69% of the current volume of desalinated water produced  
64 worldwide in 2018.<sup>25</sup> The energy to drive desalination in SWRO plants has dropped  
65 significantly over the last four decades as a result of improvements in membrane  
66 technology, the installation of energy recovery systems and the use of more efficient  
67 pumps.<sup>26–28</sup> However, this technology remains an intensive-energy and costly freshwater  
68 source.<sup>27,29</sup> Indeed, the specific energy consumption (SEC) –the energy consumed per  
69 cubic meter of freshwater produced– of current state-of-the-art SWRO plants falls within  
70 the range of 2.5–6.0  $\text{kWh m}^{-3}$  depending on several site-specific factors<sup>30</sup> as feed's  
71 composition and temperature, water quality standards, brine management, production

72 capacity<sup>31,32</sup> and RO plant configuration<sup>33</sup> contributing up to 40% in the water cost of  
73 large-scale seawater desalination plants.<sup>26,34</sup>

74 The minimum theoretical energy for desalination of seawater –assuming a feed salt  
75 concentration of 35 ppt (parts per thousand) and 50% recovery rate–, is  $\sim 1.06 \text{ kWh m}^{-3}$ .

76 <sup>34</sup> Hence, alternatives for further reduce the energy demand of RO process are limited  
77 since desalination plants' size is finite and the actual separation process is  
78 thermodynamically irreversible. Given that a gradual increase of the global desalination  
79 capacity is forecasted in the coming years,<sup>29</sup> and the electric energy portfolio is still  
80 dominated by fossil fuels,<sup>35</sup> the search of sustainable renewable energy sources turns to  
81 be decisive for the previously mentioned decarbonisation.<sup>36,37</sup>

82 Currently, desalination driven by renewables is in the application and advance R&D  
83 stage. In 2009, the installed desalination plants powered by renewables was below 1%  
84 compared to the world's total capacity.<sup>36</sup> The preferred renewable energy systems to drive  
85 –primarily low-to-medium capacity ( $50\text{--}2,000 \text{ m}^3 \text{ day}^{-1}$ )– RO desalination plants are  
86 solar photovoltaic (31%) followed by wind energy (12%).<sup>36</sup> The main issue of these  
87 renewable sources is its intermittency since RO desalination requires a continuous energy  
88 supply that ensures its operability. Conversely, SGE-RED systems can provide  
89 continuous energy supply to power desalination. Research in RED has been devoted to  
90 improvements in stack design,<sup>1,38</sup> membrane development,<sup>1,39</sup> process analysis and  
91 optimization,<sup>40</sup> fouling control<sup>41</sup> and hybrid processes.<sup>1,38</sup> Lately, the progress of SGE-  
92 RED systems to pilot plant scale has boost research in control processes in SGE-RED  
93 systems.<sup>11,12</sup> Several works underline the synergic benefits of SGE-RED integration in  
94 membrane-based desalination processes as RO; for instance, Li et al. conceptual  
95 modelling of RED-RO hybridization, reporting the optimal operating conditions of the

96 RED process alongside different integration schemes of a RED network, indicates RED  
97 could remarkably reduce the SEC while improves rejected brine management compared  
98 to conventional SWRO.<sup>16</sup> Tufa et al. novel design which combines membrane distillation  
99 and RED to simultaneously produce water and energy from SWRO brine, supports low-  
100 energy and Near-Zero Liquid Discharge seawater desalination.<sup>22,42</sup> Although SGE-RED  
101 technology co-located with a SWRO facility can provide an evident energy relief due to  
102 the SGE retrieved from waste streams, the full environmental consequences of such  
103 concept are barely studied in the reported literature. Since all renewable energy  
104 technologies have associated environmental burdens –mainly due to the environmental  
105 amortisation of the infrastructure– it is mandatory to objectively quantify the potential  
106 environmental benefits of SGE-RED integration.

107 Life Cycle Assessment (LCA), a comprehensive and internationally well-known  
108 standardized tool to evaluate the environmental performance of products and services  
109 throughout its entire life cycle,<sup>43</sup> can help identify the hot spots of SGE-RED concept. Its  
110 use provides the decision-maker with coherent, transparent, reproducible, and  
111 quantitative information about the environmental consequences in the full life cycle,  
112 avoiding shifting burden across environmental compartments or regions. SGE-RED  
113 environmental burdens are primarily caused by the infrastructure of the stack as no  
114 relevant additional material or energy resources are needed to operate the system, likewise  
115 wind or solar energy systems. The lack of similar environmental studies may be related  
116 to the very few SGE-RED pilot projects built and operated for long periods.<sup>44–46</sup> While  
117 the LCA tool is vastly used for the environmental assessment of the energy produced  
118 from non-renewable and renewable sources,<sup>47–50</sup> to the best of our knowledge, this work  
119 presents the very first environmental assessment of the SGE-RED technology using LCA.

120 This study aims to provide relevant insight into the environmental performance of SGE<sup>New Article Online</sup>  
121 RED by quantifying its environmental burdens through an LCA study. Two study cases  
122 are assessed to characterise this technology: (i) a stand-alone RED unit (Case 1) and (ii)  
123 an up-scaled RED system integrated into a real working environment, specifically a  
124 SWRO desalination plant (Case 2). The remainder of this paper is organised as follows.  
125 Section 2 describes the methodology. We define the goal and scope, i.e. the system  
126 boundary of Case 1 and Case 2 and the source for the primary and background data used  
127 to build the corresponding life cycle inventories (LCI). The midpoint impact categories  
128 considered in the study are also justified. Section 3 presents the results for each case,  
129 examining both the LCI and the values for the chosen impact categories. Regarding Case  
130 1, we performed a sensitivity analysis of the number of cell pairs and membrane area (up-  
131 scaled stack), the degradation rate of the membranes, and the spacer material to examine  
132 their influence on the RED environmental performance. In Case 2, the environmental  
133 improvements attained in the hybrid SWRO-RED scheme are analysed and properly  
134 discussed. Specifically, the impact reduction achieved when SWRO energy demand is  
135 partly supplied by RED instead of the Spanish energy grid mix, defined as the baseline  
136 scenario. Finally, Section 4 outlines the main conclusions with some indications for future  
137 work. The findings reported here show for the first time the environmental performance  
138 of an SGE-RED system. The insights gained from this study may be of assistance to future  
139 design improvements of this technology, outlining the promising outcomes of SGE-RED  
140 implementation in energy-intensive processes.

141

142

## 143 **2. Methodology**

View Article Online  
DOI: 10.1039/D0SE00372G

### 144 **2.1. Life cycle assessment methodology**

145 The international standard series ISO 14040:2006<sup>43</sup> and 14044:2006<sup>51</sup> specify the LCA  
146 methodological framework followed in the present study, which involves four iterative  
147 phases: goal and scope definition, inventory analysis, impact assessment and  
148 interpretation.

149 The RED stack model and the analysed scenarios were implemented in the LCA software  
150 GaBi ts version 9.1 (thinkstep, Germany).<sup>52</sup> We applied an attributional process-based  
151 approach, which accounts for relevant physical flows (i.e., resources, material, energy,  
152 and emissions) attributed to the provision of a specified amount of the functional unit  
153 across a product lifecycle.<sup>53</sup>

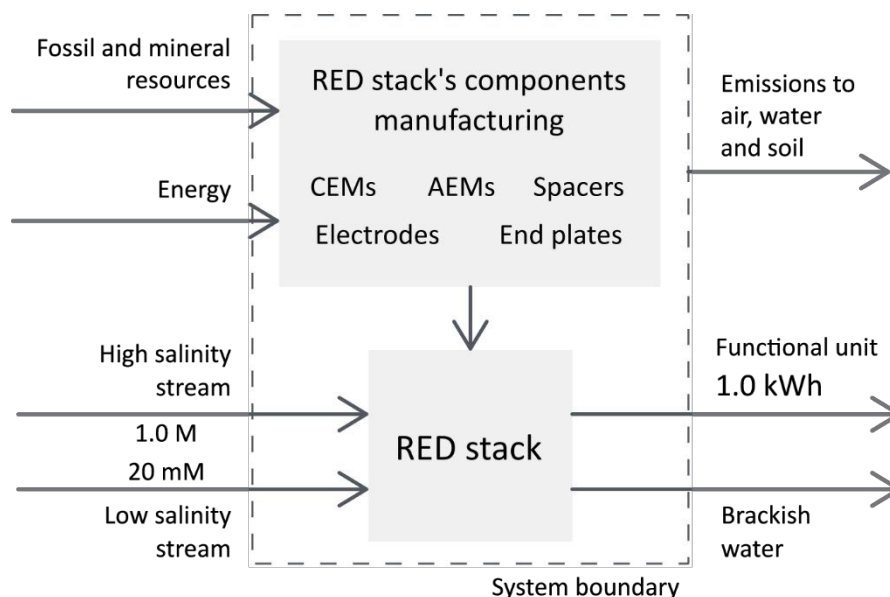
### 154 **2.2. Phase 1: Goal and scope definition**

155 The LCA was conducted in two stages, which are defined by two study cases. The goal  
156 in the first stage (Case 1) was to evaluate the environmental burdens of a stand-alone  
157 RED stack unit, to identify the “hot spots” and the potential environmental improvements  
158 of this technology and to check if the SGE-RED system is environmentally competitive  
159 compared to other renewable energy systems. The definition of the SGE-RED  
160 environmental profile enabled the assessment of its implementation in a real operation  
161 scenario in the second stage (Case 2). The goal in this phase was to quantify the emissions  
162 and the energy savings that SGE-RED could provide to energy-intensive processes such  
163 as desalination.

164

165 **2.2.1. Case 1: Stand-alone RED stack unit.**

166 The intermediate energy and materials input flows in the RED system were identified and  
 167 quantified along with the emissions released to the environment over the RED unit's life  
 168 cycle from the extraction of primary resources (such as oil or ore deposits) through the  
 169 production phase (i.e. a cradle-to-gate approach, **Fig. 1**). Then, the data collected in the  
 170 inventory analysis was translated into a set of impact indicators by characterization  
 171 models in the impact assessment phase. The impact indicators, which were referred to the  
 172 functional unit, quantified the environmental loads of the RED unit in the interpretation  
 173 phase.



174

175 **Fig. 1** SGE-RED unit's system boundary.

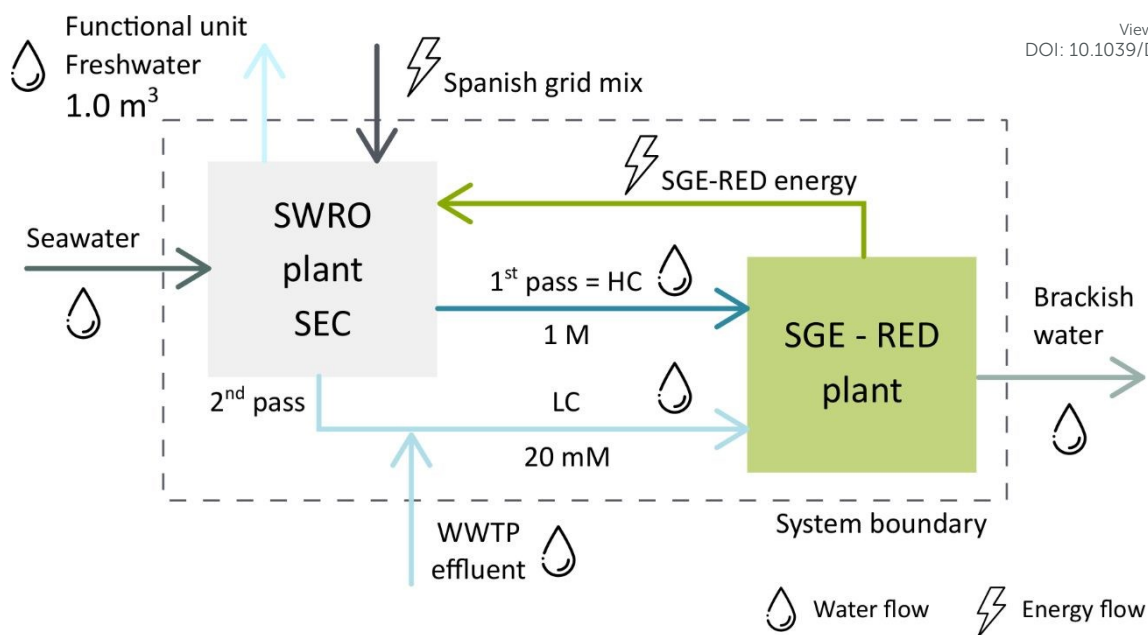
176 The assessment encompassed three distinct RED stack sizes, two lab-scale units and a  
 177 product-scale one (**Table 1**). The functional unit set in the first stage was 1.0 kWh of  
 178 gross energy yielded by each RED stack unit (**Table 1**) in the operational scenarios  
 179 reported in **Table 2** (set based on RED unit's size). The functional unit was defined

180 considering the design lifetime of the RED plant and the total electricity generated over  
181 the lifespan of the system in the different scenarios addressed in the study. The RED  
182 lifetime assumed in the assessment was 20 years.<sup>10</sup> The auxiliary equipment needed in  
183 RED operation such as pumps, pipes and electric power conversion systems and the  
184 related external energetic losses, were neglected in this part of the study according to the  
185 established cut-off criteria.

### 186 **2.2.2. Case 2. SGE-RED integration into a SWRO plant.**

187 The environmental loads per cubic meter of freshwater in the hybrid SWRO-RED  
188 scheme, i.e. the functional unit in the second stage –system boundary depicted in **Fig. 2**–  
189 were estimated assuming that RED supplies to the SWRO plant (i) the maximum  
190 extractable thermodynamic energy —the energy released in the complete mixing of the  
191 first pass SWRO concentrate effluent with the mixed stream produced by blending the  
192 second pass SWRO concentrate and the wastewater treatment plant (WWTP) effluent—  
193 ; and (ii) the actual energy output from the RED plant. The environmental loads of RED  
194 coupled with the SWRO plant were compared to the baseline scenario, where the Spanish  
195 grid mix fulfils the energy requirements of the SWRO plant. The assessment is restricted  
196 to the SWRO energy demand during the operational phase in the aforementioned  
197 scenarios. The SWRO plant's infrastructure and pretreatment of feed's streams, involved  
198 in operation phase were left out of the system boundary.

View Article Online  
DOI: 10.1039/D0SE00372G

View Article Online  
DOI: 10.1039/D0SE00372G

199

**Fig. 2** System boundary of SGE-RED integration into a SWRO desalination plant. The SGE-RED plant recovers the energy released in the controlled mix of the 1<sup>st</sup> pass SWRO concentrate and the blended 2<sup>nd</sup> pass SWRO rejected stream with the WWTP effluent to partly power desalination in place of the Spanish energy mix.

200

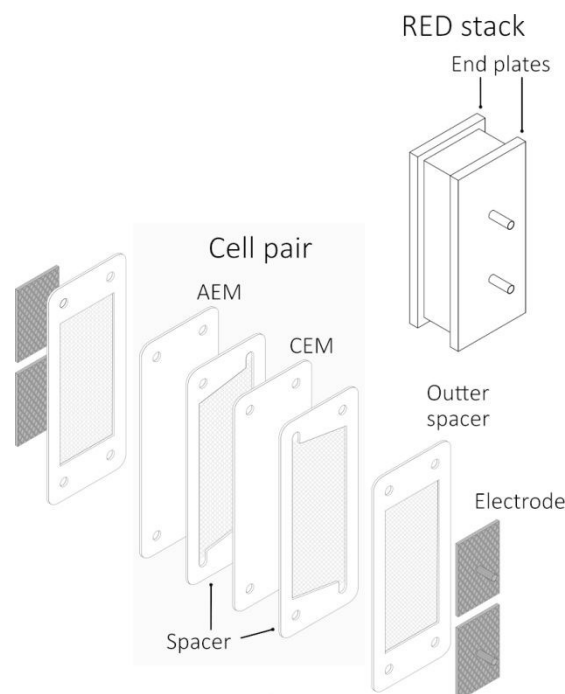
### 201 2.3. Phase 2: Life cycle inventory analysis (LCI)

#### 202 2.3.1. Case 1. Stand-alone RED stack unit.

203 The RED stack unit modelled in the assessment –depicted in **Fig. 3**– is made up of several  
 204 cell pairs each with a cation exchange membrane (CEM) and an anion exchange  
 205 membrane (AEM) kept apart by spacers. An additional cationic membrane placed next to  
 206 the electrodes shield the outer feed compartments from the electrode chambers. The net  
 207 polymer spacers are disposed between the membranes to alternatively distribute the  
 208 concentrate and diluate streams, to keep the inter-membrane distance and to provide  
 209 mechanical stability. The inlet and outlet manifolds shaped in the silicone gasket –  
 210 framing the net polymer spacers–, force the high salinity and low salinity streams to flow  
 211 through the stack in alternate channels. The cell pile is closed with an endplate on either  
 212  
 213  
 214  
 215

11

216 side and is compressed by stain-less steel bolts and nuts to limit leakages. The chambers  
 217 drilled in each endplate contains the electrodes and the flowing electrolyte solution i.e.  
 218 the electrode rinse solution recirculated over the electrode compartments.



219  
 220 **Fig. 3** RED stack's components considered in the LCA.

221  
 222 **Table 1** summarises the number of cell pairs and membrane size of the commercial RED  
 223 stack units considered in the assessment. The relevant input material flows were identified  
 224 and quantified dismantling a lab-scale module from Fumatech® (foreground data, RED  
 225 unit #1). The inventory analysis from the up-scaled RED module #3, with higher  
 226 membrane area and number of cells, was defined by extrapolation of the #1 lab-scale  
 227 RED stack inventory analysis results. The number of cell pairs of the product-scale stack  
 228 was assigned according to large-scale commercial RED stacks reported in the  
 229 literature.<sup>7,54</sup> The #2 lab-scale module is the same as the dismantled RED stack #1 except  
 230 for the number of cell pairs, which were assigned based on the maximum number of cells

231 admitted by the lab-scale module type according to manufacturer's specifications. The  
 232 membrane standard dimensions of the product-scale module were also extracted from  
 233 Fumatech®.

234 **Table 1.** Number of cell pairs and membrane size of the lab-scale and product-scale  
 235 RED stack units.

RED stack	Cell pairs	Membrane area (m <sup>2</sup> )		Membrane size (cm)	
		Effective	Total	Effective	Total
<b>Lab-scale</b>					
#1	20	0.020	0.046	6.3 x 32	10.0 x 45.8
#2	250				
<b>Product-scale</b>					
#3	1000	0.175	0.252	45.6 x 38.3	50.5 x 50.0

Inter-membrane distance: 270  $\mu\text{m}$

236

237 The lab-scale RED stack #1 (module type FT-ED-200 Fumatech®, Germany) –used to  
 238 validate the RED mathematical model<sup>40</sup>– contains 20 cell pairs. The homogeneous ion-  
 239 exchange membranes of 200 cm<sup>2</sup> active membrane area (total membrane area of 458 cm<sup>2</sup>)  
 240 and a thickness of 50  $\mu\text{m}$  were also supplied by Fumatech®. According to the information  
 241 kindly supplied by the providing company, the FKS-50 CEM base polymer is SPEEK  
 242 (sulfonated poly(ether-ether-ketone)) and the FAS-50 AEM base polymer is BPPO  
 243 (brominated polyphenylene oxide). The assumed IEMs durability was 7 years.<sup>10,55</sup> The  
 244 RED stack is also composed of 40 spacers, with two extra spacers adjacent to the anode  
 245 and cathode compartments to confine the salt solutions flow over the RED pile. The net  
 246 spacers with equal dimensions as IEMs and 270  $\mu\text{m}$  thick were made of polyethersulfone  
 247 (PES). The porosity of the spacers was 0.825.<sup>40</sup> The embedded gasket material was  
 248 silicone. A 10-year lifetime was assumed for the spacers.<sup>56</sup> The stack was also equipped  
 249 with four dimensionally stable anodes (DSA®). Both anode and cathode are stretched  
 250 titanium mesh substrates coated with ruthenium/iridium metal oxides with an area of 96.1

251 cm<sup>2</sup> and 2.6 cm thick. A loading of 10 g m<sup>-2</sup> and RuO<sub>2</sub>:IrO<sub>2</sub> ratio of 70:30 coating was  
252 assumed.<sup>57,58</sup> The electrode lifetime, 10 years, was estimated based on the current density  
253 at maximum power output conditions.<sup>58,59</sup> The endplates were assumed to be made of  
254 polypropylene (PP) and last 10 years.

255 The energy yield by the RED stack unit in the different scenarios reported in **Table 2** was  
256 estimated with the mathematical model developed by Ortiz-Imedio et al.<sup>40</sup> The RED high  
257 salinity influent corresponds to the rejected 1<sup>st</sup> pass RO brine of a SWRO desalination  
258 plant in the Mediterranean Sea. The optimum RED low salinity concentration in terms of  
259 energy density was identified with the RED mathematical model.<sup>40</sup> The maximum linear  
260 flow velocity within the concentrate and diluate compartments, i.e. 3.0 cm s<sup>-1</sup>, was  
261 assigned based on operational restrictions prescribed by the manufacturer (Fumatech®).  
262 Under this scenario (Scenario a), RED delivers higher gross power densities at the  
263 expense of a greater pressure drop within the flow channels involving increased pumping  
264 power costs<sup>60</sup>. Hence, besides this scenario, we evaluated product-scale RED operation  
265 at lower flow rates (Scenario b). In this case, we assigned the optimal concentrate and  
266 diluate cross-flow velocities in terms of RED net power –equal to RED gross power  
267 output less pumping power required to overcome the internal hydrodynamic losses–  
268 estimated with the RED model<sup>40</sup> i.e. 0.6 cm s<sup>-1</sup> and 1.2 cm s<sup>-1</sup>.

269

270

271

272

273 **Table 2.** RED stack's operational conditions under scenarios a and b.

RED stack	Scenario	$v$ (cm s <sup>-1</sup> )		Q (m <sup>3</sup> h <sup>-1</sup> )	
		HC	LC	HC	LC
#1	a	3.0	3.0	0.04	0.04
#2				0.46	0.46
#3	a	3.0	3.0	13.30	13.30
	b	0.6	1.2	2.90	5.43

HC: high concentration (1 M NaCl); LC: low concentration (20 mM NaCl)

T = 297,15 K (24 °C)

Scenario a: Maximum cross-flow velocity in the feed compartments suggested by the manufacturer Fumatech®.

Scenario b: Optimum cross-flow velocity in terms of net power density estimated with the RED model.

274

275 Background data from the modelled upstream processes were taken from research and  
 276 patent literature and the ecoinvent database 3.5.<sup>61</sup> If available, average European  
 277 conditions were assumed. Infrastructure and transport requirements were always  
 278 included. The Spanish grid mix, PV solar power plant and wind energy power plant  
 279 environmental metrics were retrieved from ecoinvent database 3.5.<sup>61</sup>

### 280 2.3.2. Case 2. SGE-RED integration into a SWRO plant

281 In this scenario (**Fig. 2**), we assumed that the SGE-RED plant was installed in a medium  
 282 to large-size two-pass SWRO desalination facility in the Mediterranean Sea (seawater  
 283 salinity ranges from 37 ppt to 40 ppt). The desalination plant operational parameters  
 284 reported in **Table 3** were set based on average values of two-pass SWRO plants in the  
 285 Mediterranean Sea reported in the literature.<sup>28,62</sup> As shown in **Fig. 2**, the RED plant's high  
 286 and low salinity influents match the 1<sup>st</sup> and the 2<sup>nd</sup> pass concentrate effluents rejected by  
 287 the SWRO desalination plant. These streams, already pretreated by the SWRO plant,  
 288 exhibits better quality conditions for RED stable operation mitigating fouling issues.  
 289 However, the 2<sup>nd</sup> pass rejected stream concentration (70 mM) is over optimum RED's  
 290 diluate influent one (20 mM). Hence, the 2<sup>nd</sup> pass SWRO rejected stream was diluted with

291 the secondary WWTP effluent (2 mM).<sup>20</sup> This measure is feasible as long as the WWTP  
 292 is located close to the SWRO plant.<sup>63</sup> The resulting mixed stream volume was 0.7 m<sup>3</sup> per  
 293 cubic meter of freshwater. The pump energy needs were considered negligible, as far as  
 294 the SGE-RED plant is installed in the SWRO plant and the two streams flow into the  
 295 RED system at enough pressure to overcome the internal pressure drop.

296 **Table 3.** Two-pass SWRO desalination plant's average operational conditions per cubic  
 297 meter of freshwater assumed in the assessment.<sup>28,62</sup>

	SEC (kWh m <sup>-3</sup> )	Recovery rate (%)	Concentrate <sup>b</sup>	
			(m <sup>3</sup> m <sup>-3</sup> )	(mol L <sup>-1</sup> )
<b>1<sup>st</sup> pass RO</b>	3.0	45	1.4	1.00
<b>2<sup>nd</sup> pass RO</b>	0.9	85	0.1	0.07
<b>Total plant<sup>a</sup></b>	4.5	42	-	-

<sup>a</sup>Including energy required for feed water intake and pre-treatment.

<sup>b</sup>Computed considering the overall RO configuration and the recovery rate of the desalination plant, as well as the product water's and feed seawater's salinity.

298

#### 299 **2.4. Phase 3: Life cycle impact assessment (LCIA)**

300 The environmental performance of the RED stack unit (Case 1) and the hybrid SWRO-  
 301 RED configuration (Case 2) was evaluated in terms of three midpoint impact indicators,  
 302 which were referred to the functional unit in each case of study: Abiotic Depletion  
 303 Potential of element resources (ADP-e) in units of mass of Sb-eq, Abiotic Depletion  
 304 Potential of fossil resources (ADP-f) in MJ and Global Warming Potential (GWP) in units  
 305 of mass of CO<sub>2</sub>-eq. These three environmental indicators were those compiled within the  
 306 impact assessment method CML 2001 (Centre of Environmental Science - Leiden  
 307 University).<sup>64</sup> The CML method restricts the assessment to early stages (midpoints) in the  
 308 cause-effect chain to limit uncertainties.

309

## 310 2.5. Phase 4: Interpretation

311 A sensitivity analysis of the RED system relevant components and parameters was  
 312 performed to assess their relative influence on the overall RED unit environmental  
 313 impact.

## 314 3. Results and discussion

### 315 3.1. Case 1. RED stack's environmental impacts

#### 316 3.1.1. Life Cycle Inventory Analysis

317 **Table 4** displays the quantities of each component in the lab-scale module (#1) and the  
 318 estimated quantities of the up-scaled modules (#2 and #3). **Table 5** shows the energy  
 319 delivered by the RED units in the operational conditions reported earlier in **Table 2**.

320 **Table 4** Inventory composition of the RED stack units.

Component	Amount			Unit	Remarks
	#1	#2	#3		
CEM	0.916	11.45	252.5	m <sup>2</sup>	Total membrane area
AEM	0.916	11.45	252.5	m <sup>2</sup>	Total membrane area
Spacer	0.368	4.397	96.69	kg	Mesh fabric and gasket
Electrode	0.038	0.038	0.165	m <sup>2</sup>	@42.65 A m <sub>electrode</sub> <sup>-2</sup>
Endplate	6.667	6.667	26.656	kg	

321

322

323

324

325

326 **Table 5** Energy yield by the commercial RED stacks in scenarios a and b View Article Online  
DOI: 10.1039/D0SE00372G

RED stack	Scenario	$P_{d,gross}$ (W m <sup>-2</sup> )	$P_{gross}$ (W) <sup>a</sup>	$E_{gross}$ (MWh)
<b>Lab-scale</b>				
#1	a	3.11	1.2	0.22
#2			15.6	2.73
<b>Product-scale</b>				
#3	a	3.03	529.7	92.8
	b	2.44	425.5	74.5

$P_{d,gross}$ : Gross power density, gross power per effective membrane area per cell pair.

$E_{gross}$ : Gross energy yield per 20 years of operation (LT), operating 8760 h year<sup>-1</sup> ( $E_{gross} = P_{gross} \cdot LT \cdot Operational\ hours$ ).

<sup>a</sup>Estimated with the RED's mathematical model.<sup>40</sup>

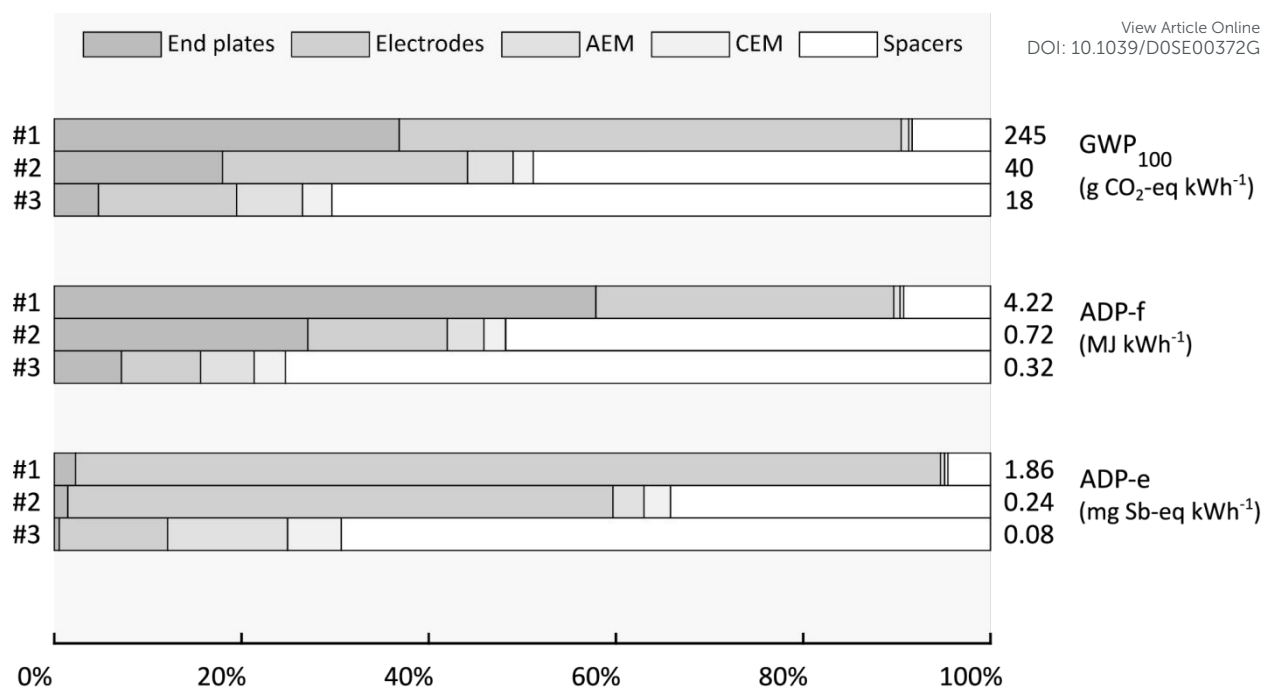
327

### 328 3.1.2. Influence of SGE-RED scaling-up

329 **Fig. 4** displays the RED stack's components contribution in the three impact categories  
 330 according to the number of cell pairs and membrane area of the lab-scale RED stacks #1  
 331 (20 cells) and #2 (250 cells) as well as the product-scale RED unit i.e. #3 (1000 cells and  
 332 larger membrane area per cell pair). **Fig. 4** also shows the aggregated value of each  
 333 indicator.

334 Regarding the lab-scale RED units, under equal operational conditions, the stack with a  
 335 greater number of cells (RED unit #2) performs better than the one with fewer cells (RED  
 336 unit #1) relating to the environmental burdens of the system. The effect of cell pair  
 337 increase is twofold: (i) a proportional increase of the energy yield since the gross power  
 338 density (i.e. the gross power per cell pair per membrane area) is equal in both systems  
 339 and (ii) a greater share of the spacers in the three impact categories. The higher energy  
 340 output of the 250-cells RED unit outweighs the environmental burdens derived from the  
 341 increased number of IEMs and spacers, representing a decline of ~83% in GWP and ADP-  
 342 f and ~87% in ADP-e. Concerning the RED stack's components contribution in the

343 impact categories, the overall environmental impact of the RED stack #1 is governed by  
344 the electrodes and endplates contributing up to ~90% to ~95% in the three impact  
345 indicators. The impact contribution is shifted to the spacers when the number of cells is  
346 increased. The spacer's share in GWP, ADP-f and ADP-e moves from ~8%, ~9% and  
347 ~5% to ~49%, ~52% and ~34% when the number of cells is twelvefold. A focus on the  
348 environmental loads of the lab-scale units' key contributors –i.e. the electrodes and the  
349 spacers in RED units #1 and #2– indicate the environmental loads exerted by a spacer  
350 (0.09 kg CO<sub>2</sub>-eq, 1.92 MJ, and 3.95·10<sup>-7</sup> kg Sb-eq) are much lower than the ones of an  
351 electrode (3.59 kg CO<sub>2</sub>-eq, 36.61 MJ, and 4.69·10<sup>-7</sup> kg Sb-eq). Therefore, increasing the  
352 number of cells offset the environmental loads of the system due to the higher energy  
353 production and the relative contribution of the spacers in the 250-cells RED unit.  
354 Although the up-scaled unit #3 requires larger absolute quantities of each component the  
355 environmental performance is also improved. The energy output counterbalances the  
356 environmental loads of the product-scale RED unit manufacture. Employing a greater  
357 number of cell pairs and membrane size leads to a ~30%, ~35% and ~42% saving in  
358 GWP, ADP-f, and ADP-e respectively comparing to the lab-scale unit #2. Overall, these  
359 results denote the need for scaling-up to drive a cleaner development of SGE-RED  
360 technology.



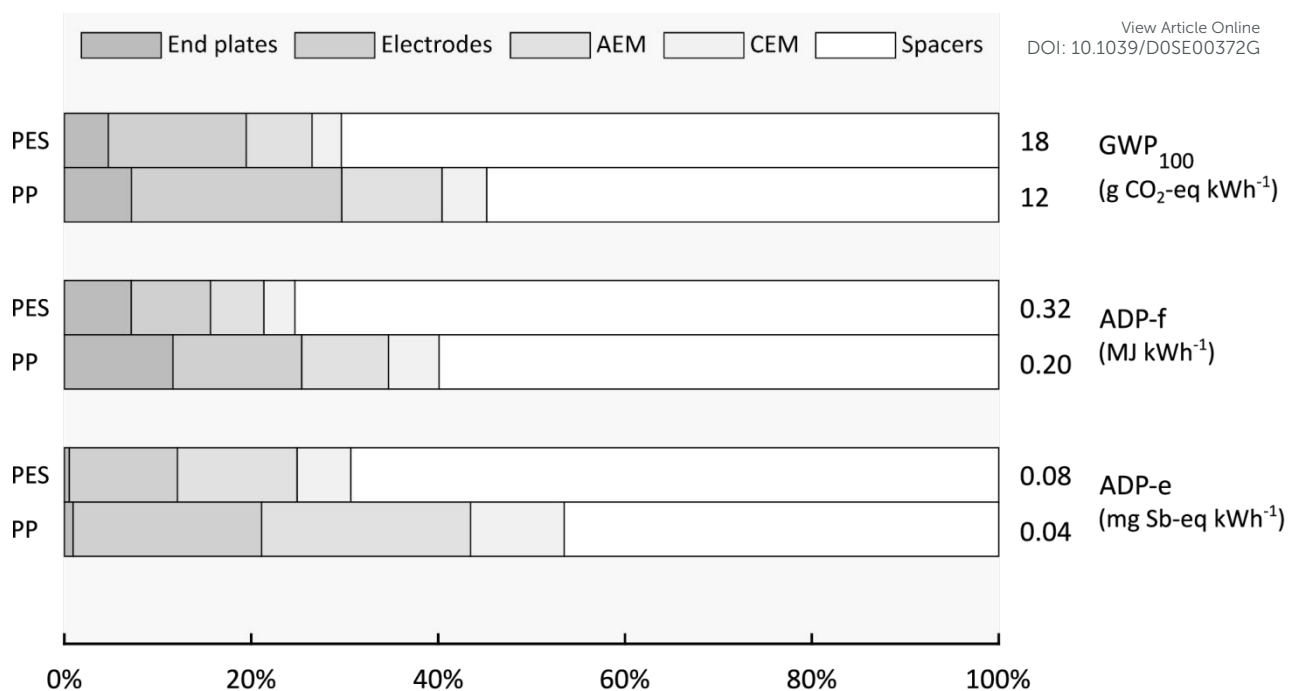
361

362 **Fig. 4** Influence of SGE-RED scaling-up: Contribution breakdown of the #1, #2 and #3  
 363 RED stacks components in GWP, ADP-f and ADP-e and their aggregated value.

364

### 365 3.1.3. Product-scale module: Influence of the spacer material

366 Previous results highlighted the spacers' dominant influence on the total environmental  
 367 profile of the RED system as the number of cells was increased. Hence, we carried out a  
 368 detailed environmental load analysis of the spacer's components i.e. the gasket and the  
 369 mesh fabric. The environmental metrics of each process and materials required in the  
 370 spacer manufacture was retrieved from ecoinvent database. Examining the impact  
 371 breakdown of a spacer, over half of the impact is caused by the fabric material (i.e.  
 372 polyethersulfone, PES) followed by the gasket material. Consequently, we set different  
 373 materials to the product-scale RED unit spacers' fabric to analyze the potential  
 374 environmental enhancement in SGE-RED technology in contrast to PES. Specifically,  
 375 polypropylene (PP) as it exerts a reduced environmental load compared to other polymer  
 376 alternatives suitable for RED operation.<sup>65</sup>



378 **Fig. 5.** Influence of the spacer fabric material. Relative contribution of the product-scale  
 379 RED stack's components in GWP, ADP-f and ADP-e and their aggregated value. (RED  
 380 stack #3: 1000 cell pairs and effective membrane area per cell pair 0.175 m<sup>2</sup>).

381

382 **Fig. 5** presents the product-scale RED components share in the three impact categories,  
 383 as well as the total environmental metrics' value. As the bar chart show, replacement of  
 384 PES by PP could cut down GWP, ADP-f and ADP-e by ~34%, ~38% and ~43%  
 385 respectively. These results prove the effectiveness of LCA to assist RED ecologically  
 386 aware design.

### 387 3.1.4. Product-scale module: Influence of IEMs degradation rate

388 The IEMs robustness against fouling events, which depend on feed water's composition,  
 389 will determine SGE-RED deployment.<sup>66–68</sup> IEMs are the most prone to fouling among  
 390 RED stack components.<sup>67,69</sup> Hence, to consider the effect of fouled IEMs on RED  
 391 performance, we assume an annual decline in RED power output of 5%.<sup>55</sup> It is also  
 392 assumed that RED system initial power output is recovered when membranes are

393 replaced. It should be noted the assumed degradation rate is a conservative value  
394 determined by membrane properties and feed water composition.

395 **Table 6.** Influence of IEMs degradation in the product-scale RED gross energy yield  
396 and the three impact indicators.

	$E_{\text{gross}}$ (MWh)	$\text{GWP}_{100}$ (g CO <sub>2</sub> -eq kWh <sup>-1</sup> )	ADP-f (MJ kWh <sup>-1</sup> )	ADP-e (mg Sb-eq kWh <sup>-1</sup> )
No degradation	92.8	18	0.32	0.075
IEMs degradation <sup>a</sup>	79.3	21	0.37	0.088

<sup>a</sup>Assuming a 5% RED power decline per year and a full recovery of the RED initial power output with every IEMs replacement (lifetime 7 years).

397

398 IEMs degradation impairs the environmental profile of SGE-RED technology since it  
399 hinders the energy delivered by the RED system under equal operational conditions. As  
400 **Table 6** show, a 5% yearly decline in RED power leads to a ~15% full-life time energy  
401 loss. This energy drop causes a ~17% increment in all impact categories as their value is  
402 inversely proportional to RED energy delivered over its lifetime. These figures signify  
403 the relevant influence of SGE-RED long-run performance in the sustainability and  
404 feasibility of this technology.

### 405 3.1.5. SGE-RED stack environmental profile vs. other renewable energy systems

406 The three environmental metrics of the product-scale RED unit are compared to other  
407 renewable energy systems to assess RED's environmental competitiveness.

408 **Table 7** reports the environmental burdens of high voltage electricity production by a  
409 solar PV power plant and a wind power plant within the Spanish context as defined in the  
410ecoinvent database along with the product-scale RED unit ones. Additional widely  
411 accepted references are also included for solar PV and wind power systems.

412 **Table 7** Environmental impacts associated with electricity delivery to the grid from  
 413 solar photovoltaic and wind power systems and the energy delivered by the product-  
 414 scale RED unit.

	<b>GWP<sub>100</sub></b> <b>(g CO<sub>2</sub>-eq kWh<sup>-1</sup>)</b>	<b>ADP-f</b> <b>(MJ kWh<sup>-1</sup>)</b>	<b>ADP-e</b> <b>(mg Sb-eq kWh<sup>-1</sup>)</b>	<b>Reference</b>
<b>Solar PV</b>	68	0.71	1.87	ecoinvent <sup>a</sup>
	6–58 <sup>b</sup>	-	-	UNEP (2016) <sup>70</sup>
	2.9–20.7 <sup>c</sup>	-	-	Pehl et al. (2017) <sup>71</sup>
	15–90 <sup>d</sup>	-	-	Miller et al. (2019) <sup>72</sup>
<b>Wind</b>	14	0.16	0.03	ecoinvent <sup>e</sup>
	6–11 <sup>f</sup>	-	-	UNEP (2016) <sup>70</sup>
	3.3–6.3 <sup>c</sup>	-	-	Pehl et al. (2017) <sup>71</sup>
	5.0–6.0 (Onshore) 7.8–10.9 (Offshore) <sup>g</sup>	-	-	Bonou et al. (2016) <sup>73</sup>
<b>SGE-RED</b>	18	0.32	0.08	This work

<sup>a</sup>electricity production, photovoltaic, 570 kWp open ground installation, multi-Si – ES (ecoinvent 3.5). Reference year: 2014.

<sup>b</sup>Functional unit: 1.0 kWh produced in Europe. Minimum and maximum values for 6 different PV technologies under 2010 and 2050 scenarios.

<sup>c</sup>Based on the integrated assessment method REMIND. Global 2050 average of lifetime emissions over lifetime electricity production for capacities built in 2050 in a 2 °C-consistent mitigation scenario.

<sup>d</sup>Functional unit: 1.0 kWh of AC electricity delivered to the grid. Maximum and minimum values of PV power systems installed in different locations for 3 different cell types. AC capacity > 1 MW. Reference year: 2015.

<sup>e</sup>electricity production, wind, 1-3MW turbine, onshore – ES (ecoinvent 3.5). Reference year: 2014

<sup>f</sup>Functional unit: 1.0 kWh produced in Europe. Minimum and maximum values for 3 different wind technologies under 2010 and 2050 scenarios.

<sup>g</sup>Functional unit: 1.0 kWh to the grid from four representative power plants in Europe. Onshore (2.3 and 3.2 MW turbine) and offshore (4.0 and 6.0 MW turbine) with 2015 state-of-the-art technology.

415

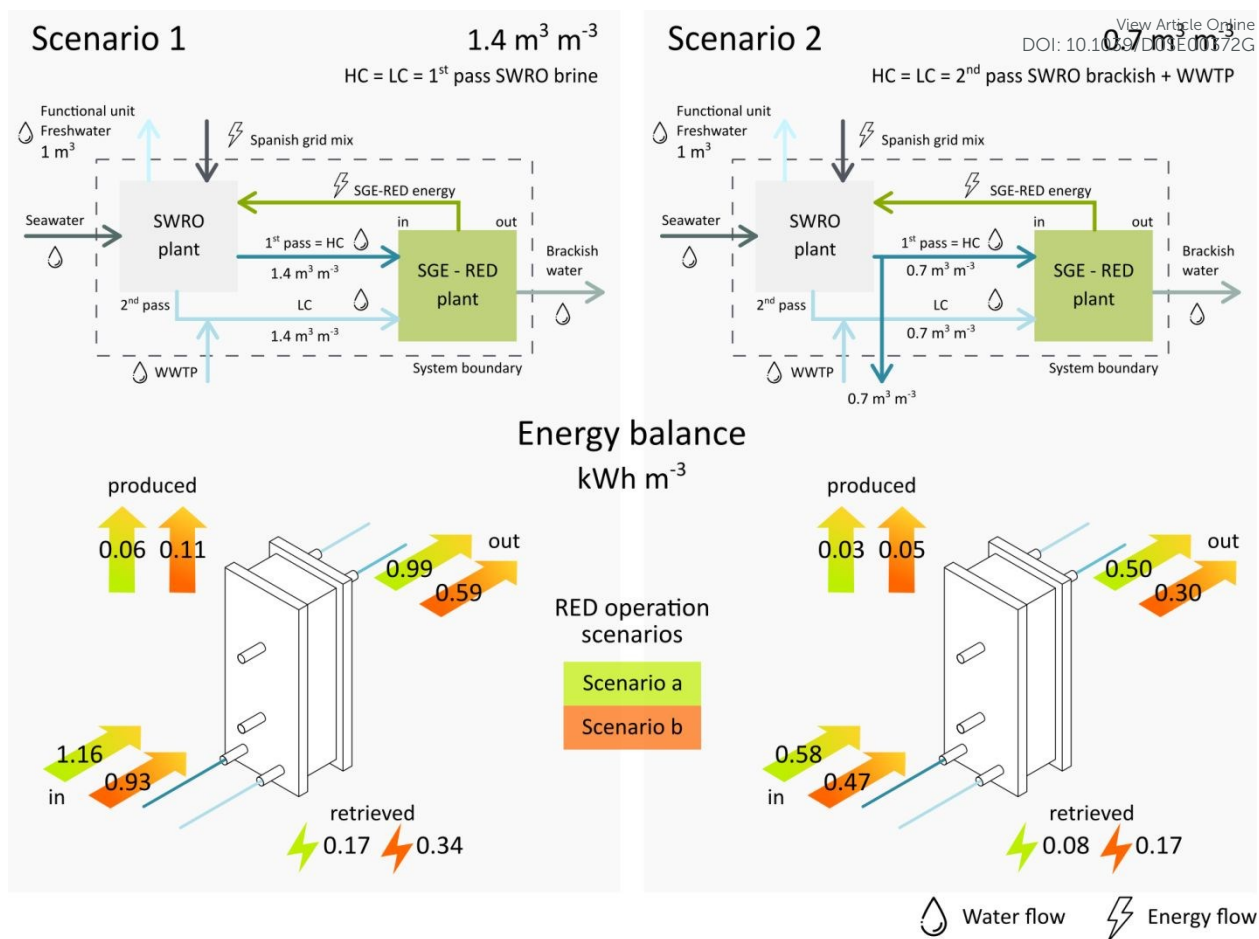
416 It must be noted that the function provided (the goal) and the scope of the assessments  
 417 are not fully equivalent. The solar PV and wind power plants' LCA is cradle-to-grave and  
 418 the functional unit is 1.0 kWh of electricity delivered to the grid whereas the function  
 419 provided in our assessment is 1.0 kWh of gross energy delivered by a RED stack under a

23

420 cradle-to-gate approach. However, as previous life-cycle assessments report, the  
421 components manufacture stage prevail in the total environmental burden of solar PV and  
422 wind power systems,<sup>70–76</sup> thus enabling a consistent comparison between the RED unit  
423 environmental loads and the ones present in these renewable energy systems. Moreover,  
424 the end-of-life stages such as RED's components recycling, and reuse could further  
425 reduce the environmental loads of the system offsetting the additional impact contribution  
426 of other life-cycle stages, side equipment and processes not accounted in the RED  
427 assessment.

### 428 **3.2. Case 2. SGE-RED integration into a SWRO plant.**

429 Case 1 results reveal SGE-RED technology could promote the transition to a low-carbon  
430 economy by recovering energy from waste streams of energy-intensive industries. To  
431 quantify the potential environmental benefits of SGE-RED in such processes, this study  
432 addresses the environmental loads avoided in a hybrid SWRO-RED configuration. The  
433 environmental loads per cubic meter of freshwater produced by the SWRO desalination  
434 plant were quantified in the following scenarios when the SWRO desalination facility is  
435 powered by (i) the Spanish electricity mix; (ii) the thermodynamic limit of the SGE-RED  
436 plant operating at (a) maximum flow rate, (b) optimum net power output flow rate; and  
437 (iii) SGE-RED plant actual power output in the scenarios (a) and (b), when the RED stack  
438 units required to power the desalination plant are in parallel hydraulic configuration, i.e.  
439 the concentrate and diluate streams are evenly fed to the RED units. The aforementioned  
440 scenarios are sketched in **Fig. 6**.



441

442 **Fig. 6** SGE-RED plant energy balance in SWRO-RED Scenarios 1 and 2 under two  
 443 different RED operational conditions i.e. Scenarios a and b. Scenario 1: equal volume  
 444 availability for concentrate and diluate RED's feed streams i.e. 1<sup>st</sup> pass brine SWRO  
 445 effluent  $1.4 \text{ m}^3 \text{ m}^{-3}$ . Scenario 2: RED's low salinity influent volume restricted by 2<sup>nd</sup> pass  
 446 brackish SWRO effluent availability, i.e. 2<sup>nd</sup> pass–WWTP mixed stream volume  $0.7 \text{ m}^3$   
 447  $\text{m}^{-3}$ . Functional unit:  $1.0 \text{ m}^3$  of freshwater. in: Gibbs free energy of mixing before RED  
 448 energy conversion; out: Gibbs free energy of mixing not recovered by RED; retrieved:  
 449 fraction of the SGE available for conversion (= in – out); produced: RED useful energy  
 450 after SGE conversion (= retrieved – RED's internal losses).

451

452 The mixing free energy per unit volume of freshwater sets the upper bound energy savings  
 453 to drive SWRO desalination.<sup>18</sup> The energy released in the complete mixing  
 454 (thermodynamic equilibrium) of the 1<sup>st</sup> pass brine SWRO effluent and the diluted 2<sup>nd</sup> pass  
 455 brackish SWRO–WWTP effluent is limited by the volume of each stream available for  
 456 SGE conversion. The SWRO 2<sup>nd</sup> pass rejected volume is far lower than 1<sup>st</sup> pass rejected

25

457 one (SGE-RED diluate volume is  $\sim 50\%$  lower), hampering SGE potential to power  
458 desalination. If same volume of diluate is accessible for energy conversion, the SGE  
459 thermodynamic limit in Scenario 1.a ( $1.16 \text{ kWh m}^{-3}$ ), i.e. maximum flow rate in the  
460 concentrate and diluate RED compartments, could reach 25.8% of SWRO energy demand  
461 ( $4.50 \text{ kWh m}^{-3}$ ) while if 2<sup>nd</sup> pass–WWTP volume is assumed, i.e. Scenario 2.a, the energy  
462 exploitable by RED is halved ( $0.58 \text{ kWh m}^{-3}$ ) accounting for 13.0% of the SWRO energy  
463 consumption. RED operation under optimum net power conditions, i.e. Scenario b,  
464 requires smaller low and high saline influents volumes ( $V_{\text{HC}}:V_{\text{LC}} = 0.58:1$ ,  $1.58 \text{ m}^3$ ) than  
465 Scenario a ( $V_{\text{HC}}:V_{\text{LC}} = 1:1$ ,  $2.00 \text{ m}^3$ ). As a result, the maximum energy RED could harvest  
466 is cut by  $\sim 20\%$  in both scenarios 1.b and 2.b, and so the upper energy bound to drive  
467 desalination.

468 Despite the Gibbs free energy in Scenario 1.b and 2.b is reduced, a greater salinity  
469 gradient energy fraction is retrieved for conversion (twice the energy consumed for  
470 conversion in Scenarios 1.a and 2.a). Providing RED efficiency<sup>77</sup>, –defined as the fraction  
471 of mixing free energy consumed converted to useful work– in both operational scenarios  
472 is almost equal ( $\sim 33\%$ ), RED working at lower flow rates supplies enhanced specific  
473 energy per  $\text{m}^3$  of freshwater produced comparing Scenario a. Regarding SGE-RED  
474 energy recovery is irreversible, –due to RED internal energy losses– the actual power  
475 production diverges from the theoretical maximum extractable work, i.e. the chemical  
476 energy stored in salinity gradients cannot be completely harnessed for useful work. Thus,  
477 the real RED power output could only meet 1.2% and 2.4% of SWRO demand in  
478 scenarios 1.a and 1.b. As mentioned earlier, considering the diluate as a limited resource  
479 (Scenario 2:  $0.7 \text{ m}^3 \text{ m}^{-3}$ ) the thermodynamic limit is halved and so the RED useful work.  
480 Therefore, RED energy supply in Scenarios 2.a and 2.b drops to 0.6% and 1.2% of SWRO

481 energy demand. Even so, a significant amount of energy remains untapped. Unused SGE  
482 leaving the RED system can be further recovered by additional RED units installed in the  
483 plant, thus closing the gap between the theoretical thermodynamic limit and the overall  
484 energy retrieved by the SGE-RED plant.<sup>78</sup> These results denote SGE-RED plant layout  
485 should be thoroughly optimised to make more efficient use of these waste streams,  
486 increasing the share of energy delivered to the SWRO plant, thus easing desalination  
487 environmental burdens.

488 As long as the Spanish electricity mix environmental indicators per kWh are higher than  
489 SGE-RED ones (**Table 8**), SWRO plant's environmental burdens are enhanced when a  
490 greater fraction of grid-based electricity supply is replaced by SGE-RED. As was stated  
491 before, under Scenario 1.a assuming a full recovery of the theoretical SGE, RED could  
492 meet 25.8% of the SWRO energy demand leading to a 24.7%, 24.1%, and 8.4% maximum  
493 decrease in GWP, ADP-f and ADP-e in contrast to the Spanish electricity mix.  
494 Conversely, in Scenario 2.a assuming a RED reversible process, the free energy of mixing  
495 available for conversion is cut in half and so the enhancement of the SWRO  
496 environmental metrics, as it is depicted in **Fig. 7**. With regards to RED operation at lower  
497 flow rates, i.e. Scenarios 1.b and 2.b, the free energy of mixing is reduced by ~20%.  
498 Therefore, the maximum SWRO burden mitigation in both scenarios is decreased  
499 accordingly in the same way as Scenarios 1.a and 2.a.

500

501

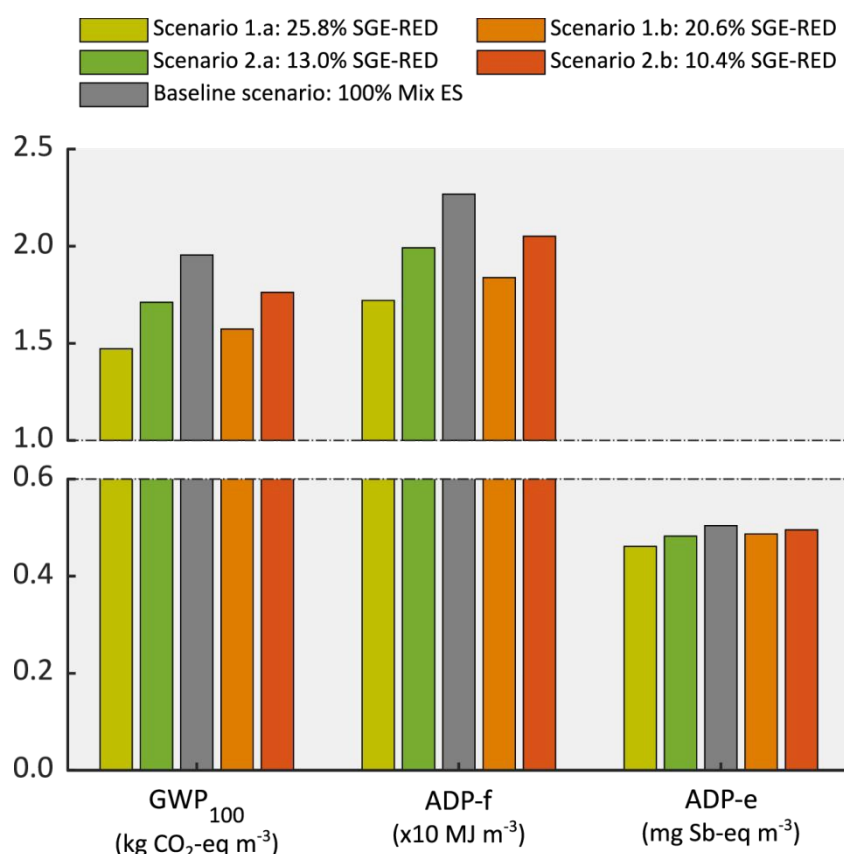
502

503 **Table 8** Environmental metrics of the Spanish electricity mix and the product-scale View Article Online  
 504 RED stack in scenarios a and b. Functional unit: 1.0 kWh DOI: 10.1039/D0SE00372G

	<b>GWP<sub>100</sub></b> (g CO <sub>2</sub> -eq kWh <sup>-1</sup> )	<b>ADP-f</b> (MJ kWh <sup>-1</sup> )	<b>ADP-e</b> (mg Sb-eq kWh <sup>-1</sup> )
<b>Spanish grid mix<sup>a</sup></b>	434	5.04	0.11
<b>SGE-RED</b>			
Scenario a	18	0.32	0.08
Scenario b	22	0.40	0.09

<sup>a</sup>Market for electricity, high voltage – ES (ecoinvent 3.5). Reference year: 2014.

505



506

507 **Fig. 7** Environmental metrics of SWRO-RED hybrid configuration in Scenario 1 and 2  
 508 under RED operation Scenarios a and b compared to SWRO desalination full-powered  
 509 by the Spanish electricity mix. Functional unit: 1.0 m<sup>3</sup> of freshwater.

510

511

512

513

514

#### 515 4. Conclusions

516 This study defines for the first time the environmental life-cycle loads of the SGE-RED  
517 technology through a cradle-to-gate LCA approach. Two study cases were assessed: (i) a  
518 stand-alone RED stack unit and (ii) SGE-RED plant integrated into a SWRO desalination  
519 plant. The mid-point environmental indicators GWP, ADP-f and ADP-e quantified the  
520 environmental loads of the aforesaid cases.

521 The first case study enabled the environmental characterisation of the RED unit. The 1<sup>st</sup>  
522 case outcomes revealed LCA as a valuable tool to assist RED design advancements. For  
523 instance, the analysis of the number of cell pairs and the membrane size influence on the  
524 three environmental metrics indicated SGE-RED scaling-up supports the sustainable  
525 development and deployment of this technology. It also assists in the identification of  
526 life-cycle RED “hot spots”. In our assessment, the main contribution to all environmental  
527 categories came from the spacers’ fabric material, which is PES. Replacement of this  
528 polymer by PP did improve the RED environmental profile. The SGE-RED’s LCA results  
529 also placed the environmental metrics of this technology within the range of other  
530 renewable power systems such as solar PV and on-shore and off-shore wind, thus proving  
531 its environmental competitiveness. Results concerning IEMs degradation impact on RED  
532 environmental performance evidenced long-term RED operation will determine the  
533 environmental feasibility of SGE-RED systems. The operation and design of a full-scale  
534 SGE-RED plant would enable an in-depth environmental load assessment of this  
535 technology under LCA framework.

536 Regarding the implementation of SGE-RED into a SWRO desalination plant, LCA results  
537 suggested SGE-RED could provide environmental benefits to the desalination sector by

538 reducing the grid mix share of its electric power demand, thus increasing the overall  
539 environmental efficiency owing to the use of available still untapped energy resources.  
540 However, SGE-RED plant layout should be optimised to increase the overall energy  
541 recovery and efficiency.

542 Overall, the RED stack's LCA may be useful in the prospective environmental decisions  
543 regarding scale-up and commercialization of SGE-RED technology. Given the spacer's  
544 relative contribution to the overall environmental burdens of the RED stack, development  
545 of spacer's novel designs and materials with anti-fouling properties and low  
546 environmental loads is needed. Improvements in membrane's properties (high  
547 permselectivity and low ionic resistance) are also relevant regarding energy efficiency  
548 and environmental profile of the RED process operating with high saline waste streams  
549 and wastewater treated effluents. Regarding RED integration in industrial processes, the  
550 systematic process synthesis and design of up-scaled RED systems to recover energy  
551 from industrial effluents are required to increase the overall process efficiency and market  
552 competitiveness.

### 553 **Conflicts of interest**

554 There are no conflicts to declare.

### 555 **Acknowledgements**

556 This work was supported by the Community of Cantabria - Regional Plan through the  
557 project Gradisal (RM16-XX-046-SODERCAN/FEDER); and the Spanish Ministry of  
558 Science, Innovation and Universities (RTI2018-093310-B-I00 and CTM2017-87850-R).  
559 Carolina Tristán is supported by the Spanish Ministry of Science, Innovation and

560 Universities (FPI grant PRE2018-086454). The authors also thank Fumatech for  
561 providing information on IEMs properties.

## 562 References

- 563 1 R. A. Tufa, S. Pawlowski, J. Veerman, K. Bouzek, E. Fontananova, G. di Profio,  
564 S. Velizarov, J. Goulão Crespo, K. Nijmeijer and E. Curcio, *Appl. Energy*, 2018,  
565 **225**, 290–331.
- 566 2 B. E. Logan and M. Elimelech, *Nature*, 2012, **488**, 313–319.
- 567 3 R. E. Pattle, *Nature*, 1954, **174**, 660–660.
- 568 4 A. Daniilidis, D. A. Vermaas, R. Herber and K. Nijmeijer, *Renew. Energy*, 2014,  
569 **64**, 123–131.
- 570 5 J. W. Post, H. V. M. Hamelers and C. J. N. Buisman, *Environ. Sci. Technol.*,  
571 2008, **42**, 5785–5790.
- 572 6 J. Veerman, R. M. de Jong, M. Saakes, S. J. Metz and G. J. Harmsen, *J. Memb.*  
573 *Sci.*, 2009, **343**, 7–15.
- 574 7 J.-Y. Nam, K.-S. Hwang, H.-C. Kim, H. Jeong, H. Kim, E. Jwa, S. Yang, J. Choi,  
575 C.-S. Kim, J.-H. Han and N. Jeong, *Water Res.*, 2019, **148**, 261–271.
- 576 8 J. Veerman, M. Saakes, S. J. Metz and G. J. Harmsen, *Environ. Sci. Technol.*,  
577 2010, **44**, 9207–9212.
- 578 9 J. Moreno, S. Grasman, R. van Engelen and K. Nijmeijer, *Environ. Sci. Technol.*,  
579 2018, **52**, 10856–10863.
- 580 10 J. W. Post, C. H. Goeting, J. Valk, S. Goinga, J. Veerman, H. V. M. Hamelers

- 581 and P. J. F. M. Hack, *Desalin. Water Treat.*, 2010, **16**, 182–193.
- 582 11 M. Tedesco, C. Scalici, D. Vaccari, A. Cipollina, A. Tamburini and G. Micale, *J.*  
583 *Memb. Sci.*, 2016, **500**, 33–45.
- 584 12 M. Tedesco, A. Cipollina, A. Tamburini and G. Micale, *J. Memb. Sci.*, 2017, **522**,  
585 226–236.
- 586 13 M. Vanoppen, S. Derese, A. Bakelants and A. R. D. Verliefde, *Desalin. Environ.*  
587 *Clean Water Energy*, 2014, 23–24.
- 588 14 Y. Mei and C. Y. Tang, *J. Memb. Sci.*, 2017, **539**, 305–312.
- 589 15 E. Brauns, *Desalin. Water Treat.*, 2010, **13**, 53–62.
- 590 16 W. Li, W. B. Krantz, E. R. Cornelissen, J. W. Post, A. R. D. Verliefde and C. Y.  
591 Tang, *Appl. Energy*, 2013, **104**, 592–602.
- 592 17 K. Kwon, J. Han, B. H. Park, Y. Shin and D. Kim, *Desalination*, 2015, **362**, 1–  
593 10.
- 594 18 N. Y. Yip, D. Brogioli, H. V. M. Hamelers and K. Nijmeijer, *Environ. Sci.*  
595 *Technol.*, 2016, **50**, 12072–12094.
- 596 19 L. Gómez-Coma, V. M. Ortiz-Martínez, M. Fallanza, A. Ortiz, R. Ibañez and I.  
597 Ortiz, *J. Water Process Eng.*, 2020, **33**, 101020.
- 598 20 J. Luque Di Salvo, A. Cosenza, A. Tamburini, G. Micale and A. Cipollina, *J.*  
599 *Environ. Manage.*, 2018, **217**, 871–887.
- 600 21 R. A. Tufa, E. Curcio, W. van Baak, J. Veerman, S. Grasman, E. Fontananova  
601 and G. Di Profio, *RSC Adv.*, 2014, **4**, 42617–42623.

- 602 22 R. A. Tufa, E. Curcio, E. Brauns, W. van Baak, E. Fontananova and G. Di Profio,  
603 *J. Memb. Sci.*, 2015, **496**, 325–333.
- 604 23 WWAP, *The United Nations World Water Development Report 2019: Leaving*  
605 *No One Behind*, UNESCO, Paris, 2019.
- 606 24 GWI and IDA, *IDA Water Security Handbook 2018 - 2019*, Media Analytics  
607 Ltd., UK, 2018.
- 608 25 E. Jones, M. Qadir, M. T. H. van Vliet, V. Smakhtin and S. Kang, *Sci. Total*  
609 *Environ.*, 2019, **657**, 1343–1356.
- 610 26 N. Voutchkov, *Desalination*, 2018, **431**, 2–14.
- 611 27 G. Amy, N. Ghaffour, Z. Li, L. Francis, R. V. Linares, T. Missimer and S.  
612 Lattemann, *Desalination*, 2017, **401**, 16–21.
- 613 28 J. Kim, K. Park, D. R. Yang and S. Hong, *Appl. Energy*, 2019, **254**, 113652.
- 614 29 U. Caldera, D. Bogdanov and C. Breyer, in *Renewable Energy Powered*  
615 *Desalination Handbook*, ed. V. Gnanaswar Gude, Butterworth-Heinemann, 2018,  
616 pp. 287–329.
- 617 30 J. R. Ziolkowska, *Water Resour. Manag.*, 2015, **29**, 1385–1397.
- 618 31 N. Ghaffour, T. M. Missimer and G. L. Amy, *Desalination*, 2013, **309**, 197–207.
- 619 32 A. Al-Karaghoulis and L. L. Kazmerski, *Renew. Sustain. Energy Rev.*, 2013, **24**,  
620 343–356.
- 621 33 C. S. Karavas, K. G. Arvanitis, G. Kyriakarakos, D. D. Piromalis and G.  
622 Papadakis, *Sol. Energy*, 2018, **159**, 947–961.

- 623 34 M. Elimelech and W. A. Phillip, *Science (80-. )*, 2011, **333**, 712–717. View Article Online  
DOI: 10.1039/D0SE00372G
- 624 35 BP Energy Economics, *BP Statistical Review of World Energy 2018*, BP p.l.c.,  
625 London, UK, 67th edn., 2018.
- 626 36 M. Isaka, *IRENA-IEA-ETSAP Technol. Br. 112*, 2013, 1–10.
- 627 37 R. Fornarelli, F. Shahnia, M. Anda, P. A. Bahri and G. Ho, *Desalination*, 2018,  
628 **435**, 128–139.
- 629 38 H. Tian, Y. Wang, Y. Pei and J. C. Crittenden, *Appl. Energy*, 2020, **262**, 114482.
- 630 39 T. R. Willson, I. Hamerton, J. R. Varcoe and R. Bance-Soualhi, *Sustain. Energy*  
631 *Fuels*, 2019, **3**, 1682–1692.
- 632 40 R. Ortiz-Imedio, L. Gomez-Coma, M. Fallanza, A. Ortiz, R. Ibañez and I. Ortiz,  
633 *Desalination*, 2019, **457**, 8–21.
- 634 41 S. Pawlowski, R. M. Huertas, C. F. Galinha, J. G. Crespo and S. Velizarov,  
635 *Desalination*, 2020, **476**, 114183.
- 636 42 R. A. Tufa, Y. Noviello, G. Di Profio, F. Macedonio, A. Ali, E. Drioli, E.  
637 Fontananova, K. Bouzek and E. Curcio, *Appl. Energy*, 2019, **253**, 113551.
- 638 43 ISO, *ISO 14040:2006: Environmental management — Life cycle assessment —*  
639 *Principles and framework*, Geneva, Switzerland, 2006.
- 640 44 C. Seyfried, H. Palko and L. Dubbs, *Renew. Sustain. Energy Rev.*, 2019, **102**,  
641 111–120.
- 642 45 M. Papapetrou and K. Kumpavat, in *Sustainable Energy from Salinity Gradients*,  
643 eds. A. Cipollina and G. Micale, Elsevier Ltd., 2016, pp. 315–335.

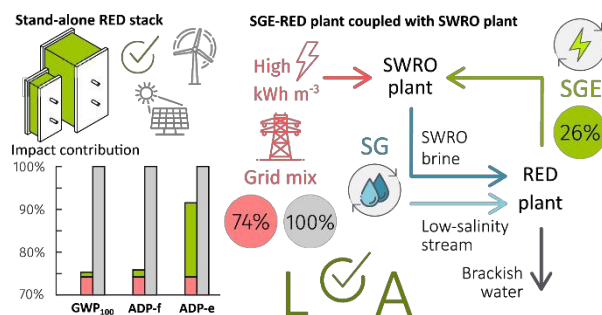
- 644 46 M. Papapetrou, G. Kosmadakis, F. Giacalone, B. Ortega-Delgado, A. Cipollina, View Article Online  
DOI: 10.1039/D0SE00372G  
645 A. Tamburini and G. Micale, *Energies*, 2019, **12**, 3206.
- 646 47 M. Margallo, A. Dominguez-Ramos, R. Aldaco, A. Bala, P. Fullana and A.  
647 Irabien, *Resour. Conserv. Recycl.*, 2014, **93**, 144–155.
- 648 48 A. Dominguez-Ramos, M. Held, R. Aldaco, M. Fischer and A. Irabien, *Int. J.*  
649 *Life Cycle Assess.*, 2010, **15**, 557–566.
- 650 49 M. V. Barros, R. Salvador, C. M. Piekarski, A. C. de Francisco and F. M. C. S.  
651 Freire, *Int. J. Life Cycle Assess.*, 2020, **25**, 36–54.
- 652 50 J. A. Alberola-Borràs, R. Vidal and I. Mora-Seró, *Sustain. Energy Fuels*, 2018, **2**,  
653 1600–1609.
- 654 51 ISO, *ISO 14044:2006: Environmental management — Life cycle assessment —*  
655 *Requirements and guidelines*, Geneva, Switzerland, 2006.
- 656 52 thinkstep, 2019.
- 657 53 G. Rebitzer, T. Ekvall, R. Frischknecht, D. Hunkeler, G. Norris, T. Rydberg, W.-  
658 P. Schmidt, S. Suh, B. P. Weidema and D. W. Pennington, *Environ. Int.*, 2004,  
659 **30**, 701–720.
- 660 54 J.-H. Han, K. Hwang, H. Jeong, S.-Y. Byeon, J.-Y. Nam, C.-S. Kim, H. Kim, S.  
661 Yang, J. Y. Choi and N. Jeong, *J. Appl. Electrochem.*, 2019, **49**, 517–528.
- 662 55 A. Daniilidis, R. Herber and D. A. Vermaas, *Appl. Energy*, 2014, **119**, 257–265.
- 663 56 H. Strathmann, *Ion - exchange Membrane separation processes*, Elsevier, 2004,  
664 vol. 9.

- 665 57 A. Y. Bagastyo, J. Radjenovic, Y. Mu, R. A. Rozendal, D. J. Batstone and K. Rabaey, *Water Res.*, 2011, **45**, 4951–4959. View Article Online  
DOI: 10.1039/D0SE00372G
- 666
- 667 58 J. Veerman, M. Saakes, S. J. Metz and G. J. Harmsen, *J. Appl. Electrochem.*,
- 668 2010, **40**, 1461–1474.
- 669 59 B. Liu, C. Wang, Y. Chen and B. Ma, *J. Electroanal. Chem.*, 2019, **837**, 175–
- 670 183.
- 671 60 D. A. Vermaas, M. Saakes and K. Nijmeijer, *Environ. Sci. Technol.*, 2011, **45**,
- 672 7089–7095.
- 673 61 G. Wernet, C. Bauer, B. Steubing, J. Reinhard, E. Moreno-Ruiz and B. Weidema,
- 674 *Int. J. Life Cycle Assess.*, 2016, **21**, 1218–1230.
- 675 62 S. Lattemann, PhD thesis, Delft University of Technology, 2010.
- 676 63 M. A. Sanz and C. Miguel, *Desalin. Water Treat.*, 2013, **51**, 111–123.
- 677 64 J. B. Guinée, M. Gorré, R. Heijungs, G. Huppes, R. Kleijn, A. de Koning, L. van
- 678 Oers, A. Wegener Sleeswijk, S. Suh, H. A. Udo de Haes, H. de Bruijn, R. van
- 679 Duin and M. A. J. Huijbregts, *Handbook on life cycle assessment. Operational*
- 680 *guide to the ISO standards. I: LCA in perspective. IIa: Guide. IIb: Operational*
- 681 *annex. III: Scientific background.*, Kluwer Academic Publishers, Dordrecht,
- 682 2002.
- 683 65 E. Van Der Burg, G. Linders, US Pat. 20180353909A1, 2018.
- 684 66 M. Vanoppen, T. van Vooren, L. Gutierrez, M. Roman, L. J.-P. Croué, K.
- 685 Verbeken, J. Philips and A. R. D. Verliefde, *Sep. Purif. Technol.*, 2019, **218**, 25–
- 686 42.

- 687 67 D. A. Vermaas, D. Kunteng, M. Saakes and K. Nijmeijer, *Water Res.*, 2013, **47**, View Article Online  
DOI:10.1039/D0SE00372G  
688 1289–1298.
- 689 68 H. Susanto, M. Fitrianingtyas, A. M. Samsudin and A. Syakur, *Int. J. Energy*  
690 *Res.*, 2017, **41**, 1474–1486.
- 691 69 T. Rijnaarts, J. Moreno, M. Saakes, W. M. de Vos and K. Nijmeijer, *Colloids*  
692 *Surfaces A Physicochem. Eng. Asp.*, 2019, **560**, 198–204.
- 693 70 UNEP, *Green Energy Choices: The benefits, risks and trade-offs of low-carbon*  
694 *technologies for electricity production.*, 2016.
- 695 71 M. Pehl, A. Arvesen, F. Humpenöder, A. Popp, E. G. Hertwich and G. Luderer,  
696 *Nat. Energy*, 2017, **2**, 939–945.
- 697 72 I. Miller, E. Gençer, H. S. Vogelbaum, P. R. Brown, S. Torkamani and F. M.  
698 O’Sullivan, *Appl. Energy*, 2019, **238**, 760–774.
- 699 73 A. Bonou, A. Laurent and S. I. Olsen, *Appl. Energy*, 2016, **180**, 327–337.
- 700 74 B. Guezuraga, R. Zauner and W. Pölz, *Renew. Energy*, 2012, **37**, 37–44.
- 701 75 M. A. P. Mahmud, N. Huda, S. H. Farjana and C. Lang, *Energies*, ,  
702 DOI:10.3390/en11092346.
- 703 76 A. Alsaleh and M. Sattler, *Clean Technol. Environ. Policy*, 2019, **21**, 887–903.
- 704 77 J. Veerman, M. Saakes, S. J. Metz and G. J. Harmsen, *J. Memb. Sci.*, 2009, **327**,  
705 136–144.
- 706 78 D. Bharadwaj and H. Struchtrup, *Sustain. Energy Fuels*, 2017, **1**, 599–614.
- 707

## Table of contents entry

View Article Online  
DOI: 10.1039/D0SE00372G



LCA of lab-scale and large-scale stand-alone RED stacks and an up-scaled RED system co-located with a SWRO desalination plant.